Supporting Information for:

A V(III)-induced metallogel with solvent stimuli-responsive properties: structural proof-of-concept with MD simulations

Sima Sedghiniya, Janet Soleimannejad*, Masumeh Foroutan*, Mina Ebrahimi and Vahid Fadaei Naeini

*Email: janet_soleimannejad@khayam.ut.ac.ir

foroutan@khayam.ut.ac.ir

Table of Contents:

I. Optimizing the preparation conditions of VGel

Since the synthesis of VGel metallogel seemed to require some optimization, several experiments were carried out according to the changes described as following tables:

1. *Temperature key factor experiments:*

Test code	T (˚C)	Gel efficiency* (%)	Description
11	70	15	Green precipitation with gel
12	80	85	-
13	90	83	-
14	100	79	-
15	110	80	Gel with orange crystals

* efficiency = weight of formed gel.100/ total weight of reactants

2. *Heating-time key factor experiments:*

Test code	Time (hours)	Gel efficiency (%)	Description
21	12	51	Gel with green precipitation
22	16	57	Gel with green precipitation
23	18	75	-
24	20	84	-
25	22	85	-
26	24	84	-

3. *Cooling-rate key factor experiments:*

Test code	Cooling-rate (˚C /min)	Gel efficiency (%)	Description
31	Oven just turned off	85	-
32	2	76	-
33	5	77	-
34	10	75	-

4. *Components' key factors experiments:*

In this section all the experiments were carried out in the absence of each components as following table:

Test code	Gel preparation in the absence of …	Description
41	Adenine	Unstable gel
42	BTC	Clear solution
43	$VOSO_4$	White precipitation
44	H_2O	White and green precipitation
45	DMF	White and green precipitation

In summary, according to the results of the above experiments, it appears that all the components $VOSO_4$, 1,3,5-benzentricarboxylic acid, Adenine, H_2O, and DMF, are critical for the production of the reported vanadium metallogel. Overall, the optimized conditions are concluded at 80 ˚C for 20 hours with no regular cooling-rate program.

II. Computational details.

H_3BTC, adenine and, $V_2(SO_4)_3$ molecules were randomly dispersed at concentrations 3.0, 2.5 and, 2.5 M respectively in the solvent mixture of H_2O/DMF by using packmol [S1]. In order to determine the contribution of each component of the solvent mixture in the gelation and also to distinguish the formation of the robust metallogel in the molecular dynamics approach by comparison, three systems with the different H_2O/DMF ratios in the solvent mixture are investigated. In the following, aforementioned systems with 71.43:28.57, 50:50 and, 28.57:71.43 v/v % H_2O/DMF are denoted as MG1, MG2 and, MG3 in order. Initially, the simulation of systems was performed for 35 ns at 410 K (high temperature), afterwards we decreased the temperature to 310 K and all systems were simulated for 40 ns at this ambient condition. Table S2 represents the number of each component used in the three systems in detail.

Moreover, equilibrated systems that were prepared by the previous simulation have been pulled under the external force with the constant velocity of 1 Å/ns for 40 ns with a focus on studying mechanical properties. A number of molecules in specified thick layers (~2Å), located at the top and bottom of the system along the Z axis, were selected. The first chosen layer at the bottom of the simulation box was fixed and an external force with constant velocity along the positive direction of the Y axis was applied to the second layer at the top of the simulation box. In the constant velocity SMD, the harmonic constant was considered 1 kcal/mol.Å^2. In Fig. 1, the initial configuration of the system is depicted in particular.

Table S1. Lennard-Jones parameters for vanadium (ш) sulfate ($V_2(SO_4)_3$) and their partial charges [S2-S4].

Atom	σ (Å)	ε (kcal/mol)	q (a.u.)
V	2.4950	0.0128	+3.0
S	3.5500	0.2500	+2.4
O	3.1500	0.2500	-1.1

Table S2. The simulation box dimension and the number of molecules of each component used in the MG1, MG2, and MG3 systems.

System Acronym	The number of molecules*						Box dimension (Å) [d_X, d_Y, d_Z]**
	H_3BTC	Adenine	V^{3+}	SO_4^{2-}	DMF	H_2O	
MG1	63	54	54	81	231	2499	[57.44, 55.87, 56.02]
MG2	63	54	54	81	409	1750	[57.25, 57.67, 56.33]
MG3	63	54	54	81	584	1000	[57.87, 57.44, 56.83]

*We only changed the number of solvents (DMF and H2O), and the number of the rest of the molecules is the same in all three systems.

** The d_X, d_Y, and d_Z show the simulation box dimension in the direction of the X, Y, and Z axes, in order.

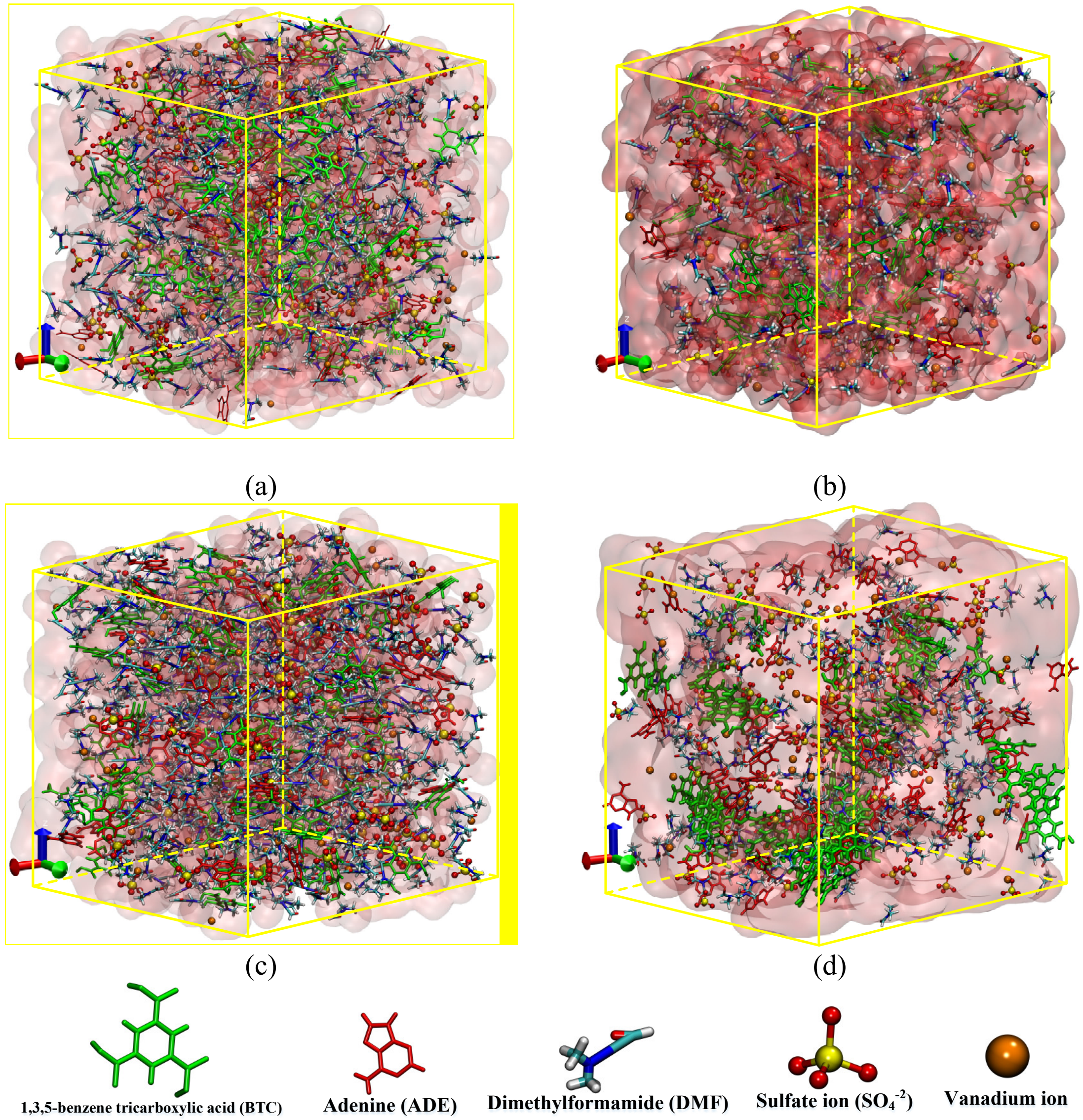

Fig. S1. The initial configurations of the MG1 (a) and MG2 (c) systems together with the final configurations of the MG1 (b) and MG2 (d) after 80 ns (water is shown in quick surface representation). Different components including BTC, adenine and DMF molecules, V^{3+} and sulfate ions (e).

III. Molecular dynamics simulation

For more evaluations the formation of our metallogel network, in all simulated systems, including MG1, MG2 and MG3, five V^{III} ions were randomly marked and their 2D trajectories (under ambient conditions in the last 4 ns of simulation time) were traced in XY plane (Fig. S2). As shown in Fig. S2, by Comparing 2D trajectories of V^{III} ions in all the simulated systems, it can be concluded that more restriction in the MG3 system indicate the formation of the gel network.

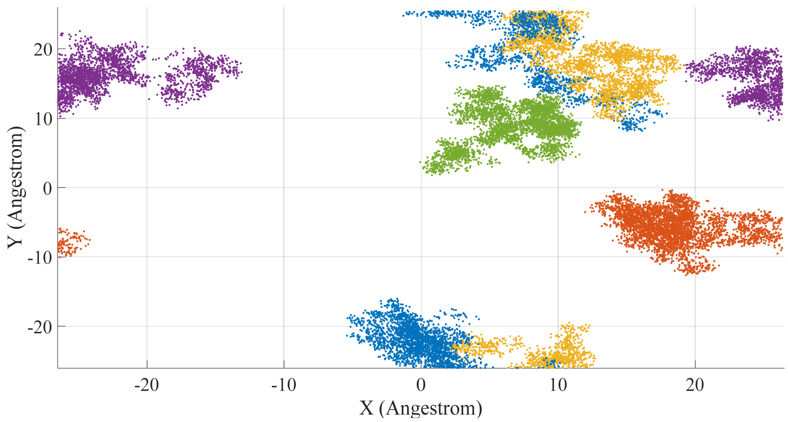

(a)

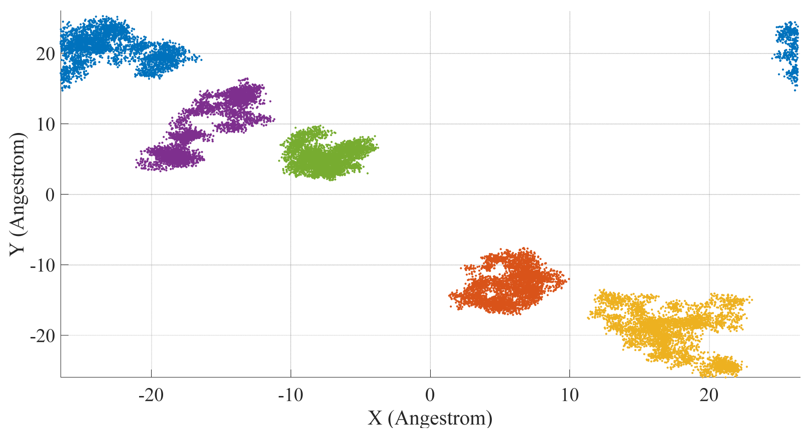

(b)

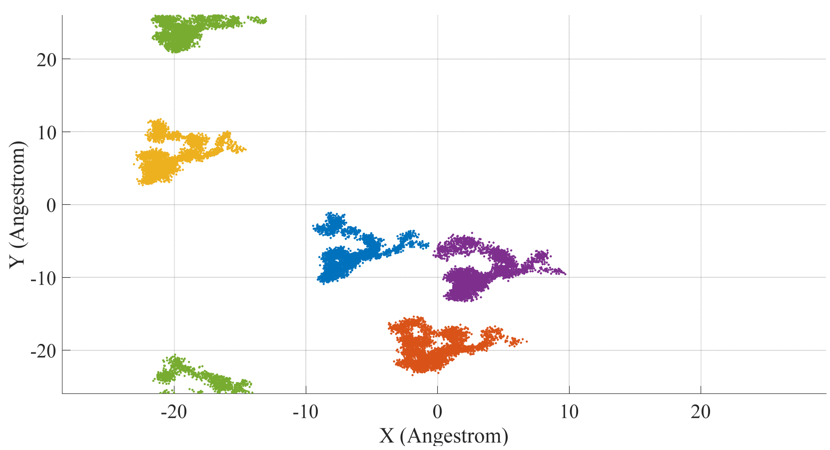

(c)

Fig. S2. 2D trajectories in the XY plane of the marked V^{III} ions in the (a) MG1, (b) MG2, and (c) MG3 systems under ambient conditions

For all simulated systems, the time evolution of the VDW and electrostatic interactions between V^{III} ions, and H_2O, DMF, BTC, and adenine molecules are presented in Fig. S3 and S4.

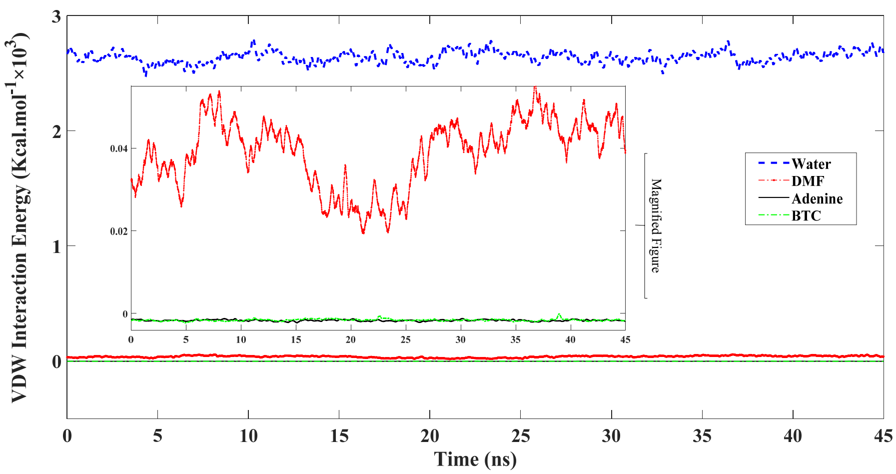

(a)

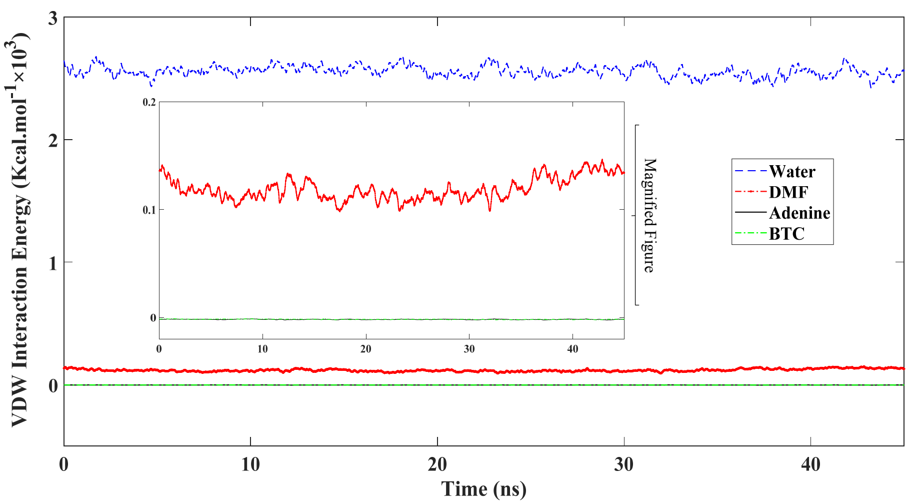

(b)

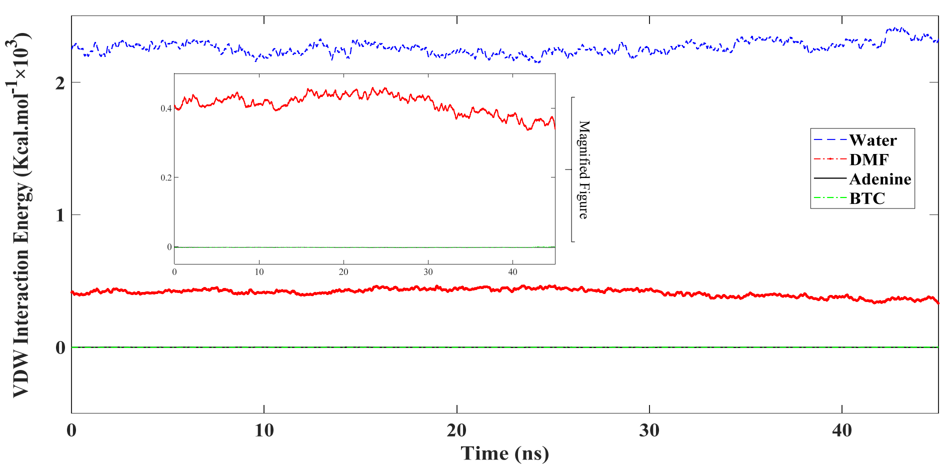

(c)

Fig. S3. The Van der Waals (VDW) interaction energies between V^{III} ions and the other components in (a) MG1, (b) MG2, and (c) MG3 systems under ambient conditions.

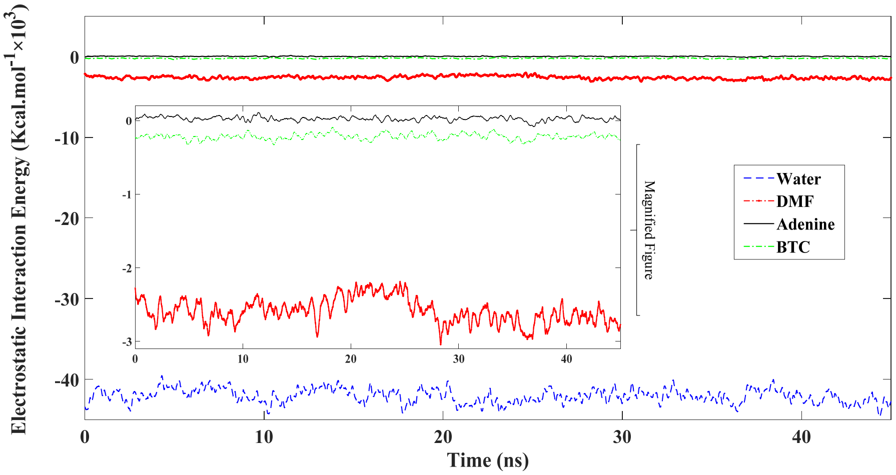

(a)

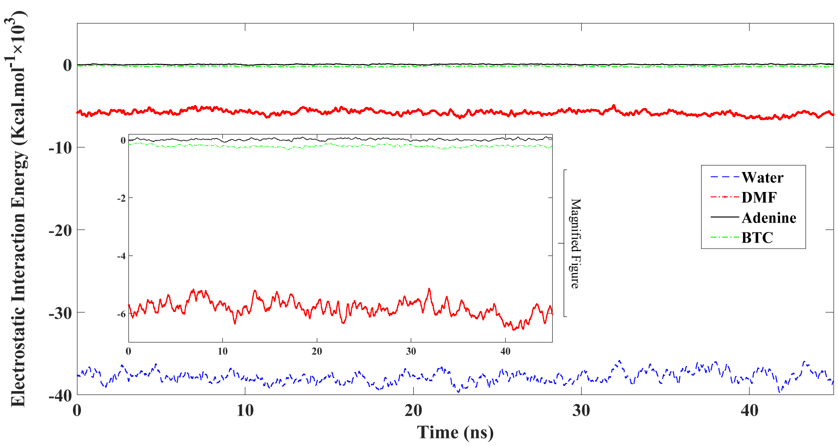

(b)

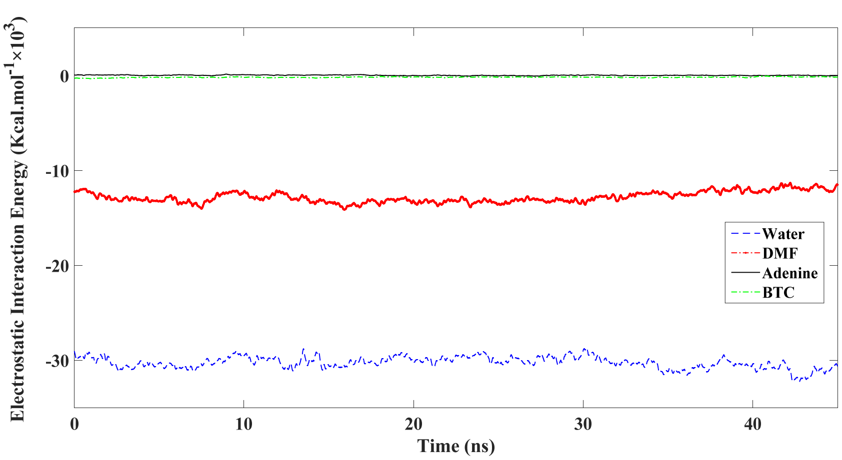

(c)

Fig. S4. The electrostatic interaction energies between V^{III} ions and the other components in (a) MG1, (b) MG2, and (c) MG3 systems under ambient conditions.

In the MG3, a system with a more robust metallogel, the accumulation of gelator molecules, especially Ade, in the first neighboring layers of the V^{III} ions is higher (Fig. S5). The gelator molecules aggregated in farther neighboring layers of the V^{III} ions than solvent components, comparing Fig. 3 and Fig. S5. In Fig. S5 the better ordering of the gelator molecules' peaks in MG3 than MG1, in confirmation of Fig. 3, represents the better arrangement of π-π stacked gelator molecules around the V^{III} ions.

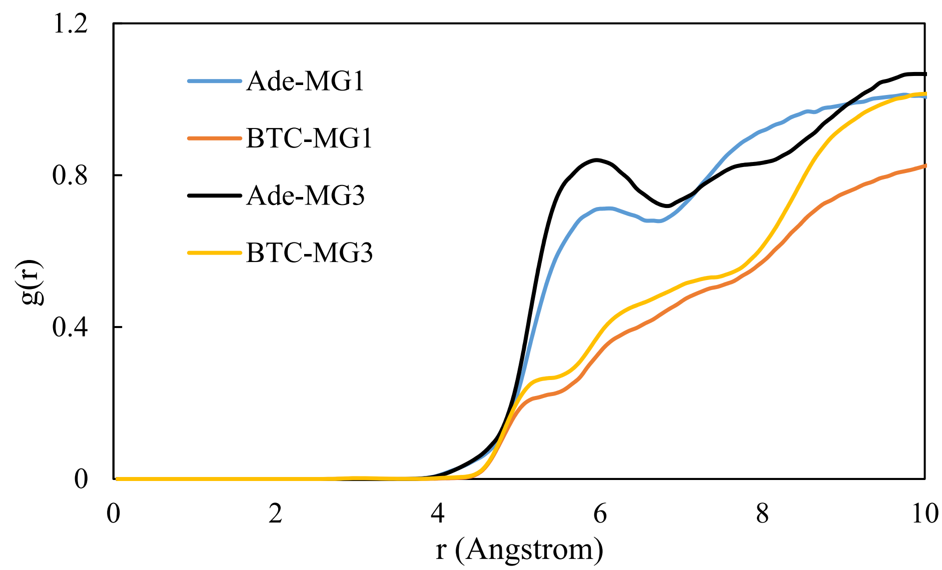

Fig. S5. RDFs between V^{III} ions and gelator molecules (BTC and Ade) at room temperature, in MG1 and MG3 systems.

The π-π stacking between BTC and BTC-adenine molecules (at room temperature), in the MG1 and MG3 systems are represented in Fig. S6 and S7, respectively. The geometric criteria of the separation of 3.6 to 4.2 Å between aromatic ring centroids of two adjacent H_3BTC or H_3BTC and adenine molecules are used to identify the π-π interaction [S6-S7].

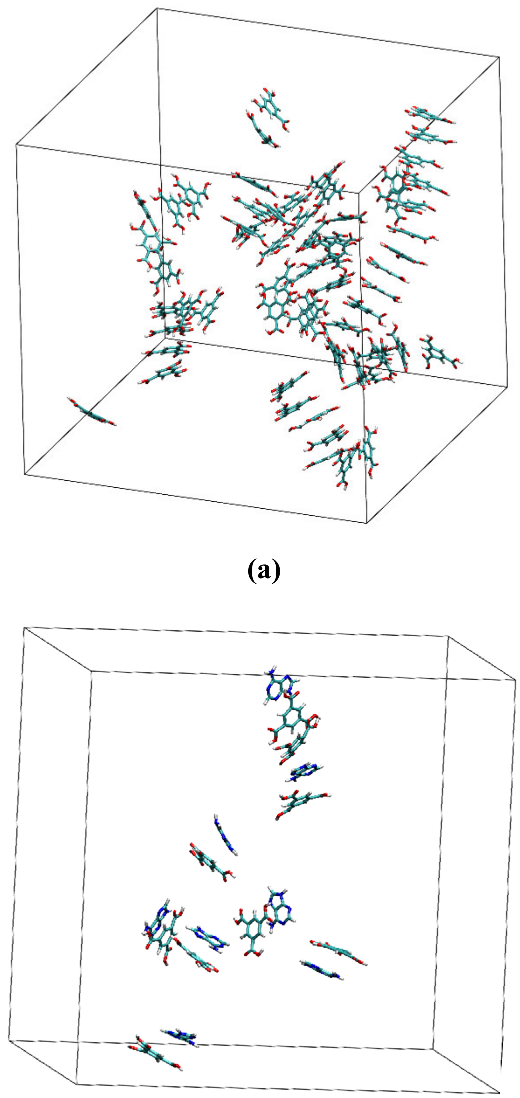

(a)

(b)

Fig. S6. The snapshot of the π-π stacking between (a) BTC and (b) BTC-adenine molecules for the MG1 system under ambient conditions.

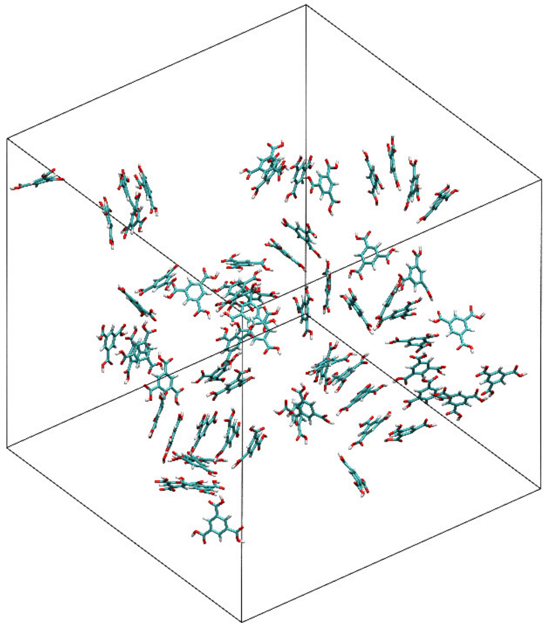

(a)

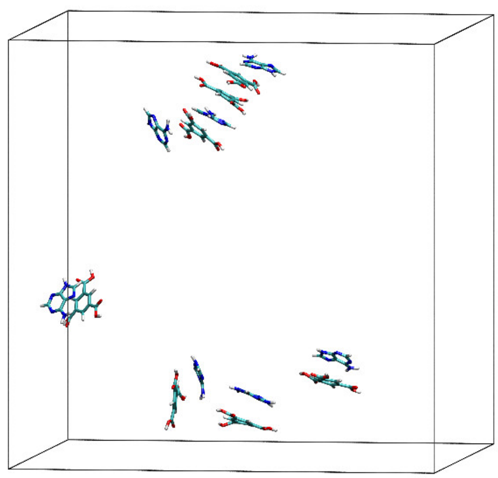

(b)

Fig. S7. The snapshot of the π-π stacking between (a) BTC and (b) BTC-adenine molecules for the MG3 system under ambient conditions.

All the simulated systems were exposed to shear stress along the positive direction of the Y axis and the initial/final configurations for each case are showed in Fig. S8.

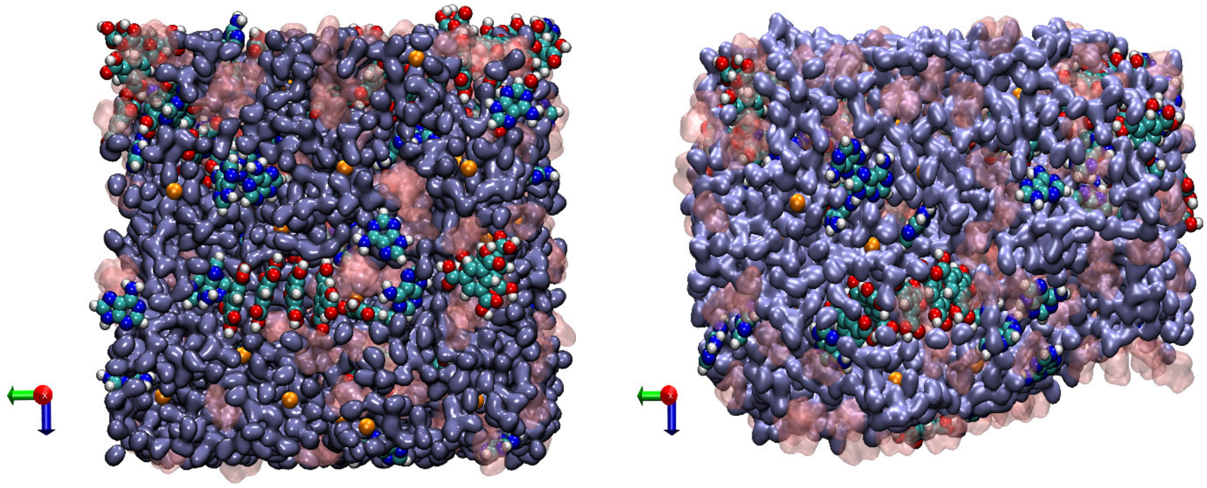

a

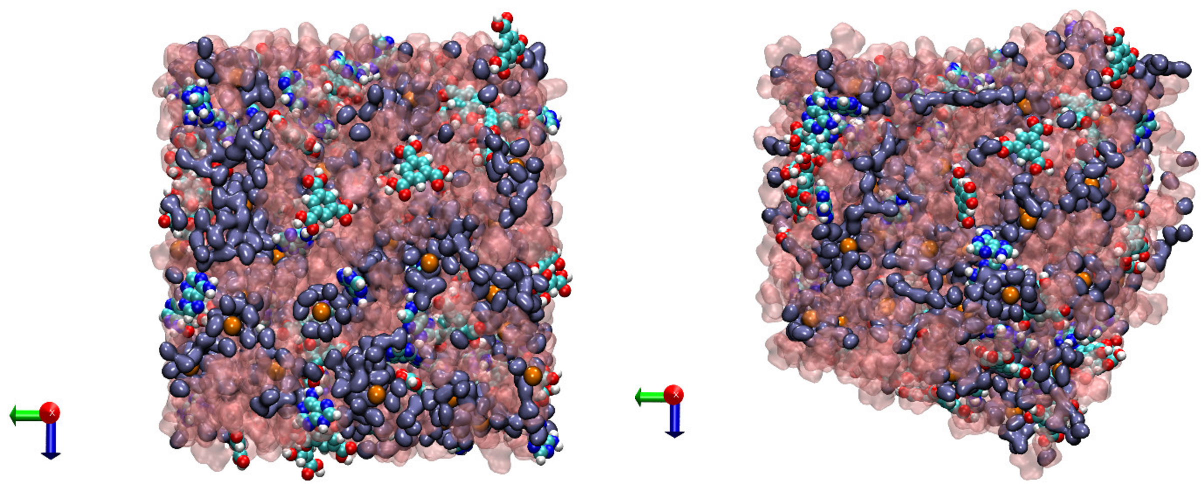

b

Fig. S8. The snapshots of the influence of shear stress loading along the Y axis in (a) MG1 and (b) MG3 systems (left side the initial and right side the final configuration).

IV. VGel characterization

Infrared spectroscopy

As we know, infrared spectroscopy (IR) is a simple and reliable technique that can be used to characterize gels, we studied IR spectra of VGel and its component, to provide an insight into the assembly of molecular-scale building blocks and responsible non-covalent interactions for gelation [S7]. According to Fig. S9, although some of BTC molecules were deprotonated to neutralize the overall charge of the resulted metallogel it appears that all the VGel components are assembled through non-covalent interactions.

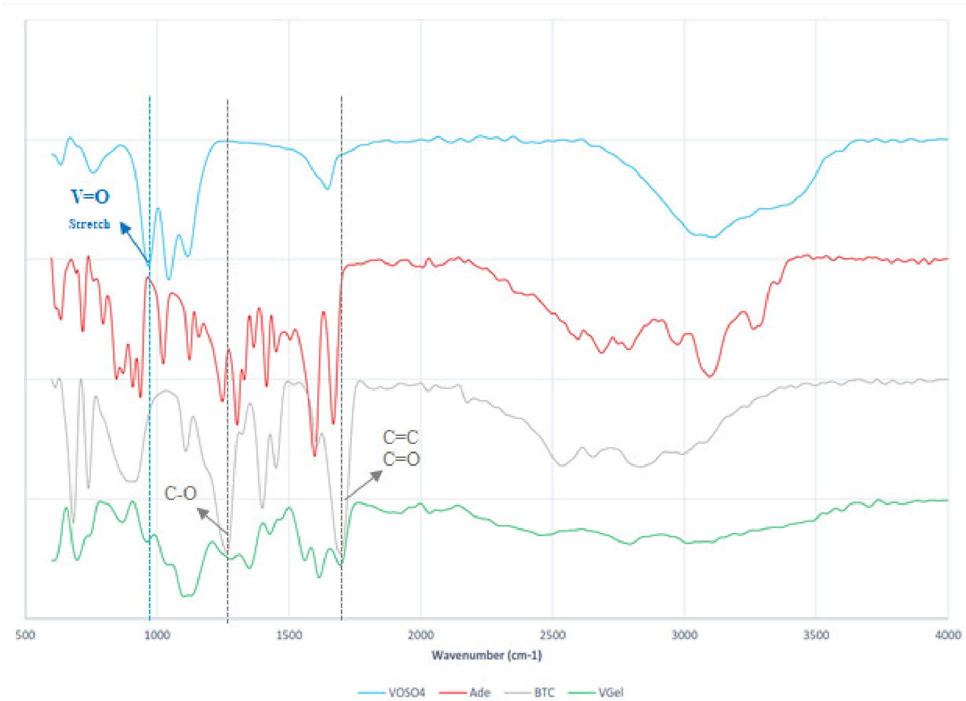

Fig. S9. FTIR spectra for the VGel and its reactants

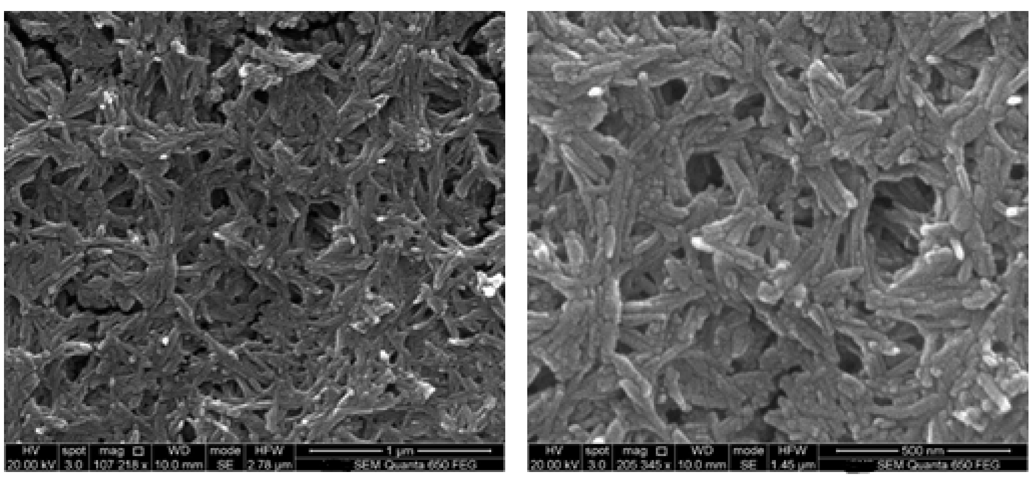

Fig. S10. SEM micrographs of the VGel

UV-Visible spectroscopy

As vanadium ions exhibit an engaging distinctive color changes (V^{II}:violet, V^{III}: green, V^{IV}: blue, and V^{V} yellow) according to the oxidation state, UV-Visible spectroscopy can provide a finger print for vanadium ions. Typical UV-Visible spectrum of VGel (in 1% aqueous concentration) was recorded (Fig. S11 and S12). The transition states, including v_1 = 400nm, v_2 = 581 nm, and, v_3 = 266 nm, were according to previous reports for solvated V^{III} (d^2). The absorbance peak at 581 nm was selected for the quantitative analyses (v_3 according to $^3T_{1g}$ (F) $^3A_{2g}$ falls in UV and is not shown in Fig. S11) [S8-S10].

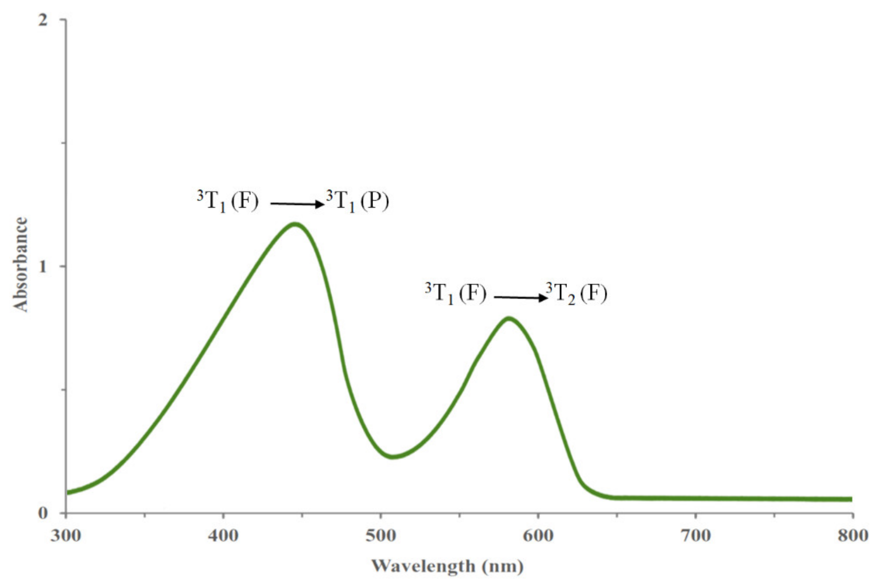

Fig. S11. The UV-Visible absorption spectrum of VGel [S8-S10]

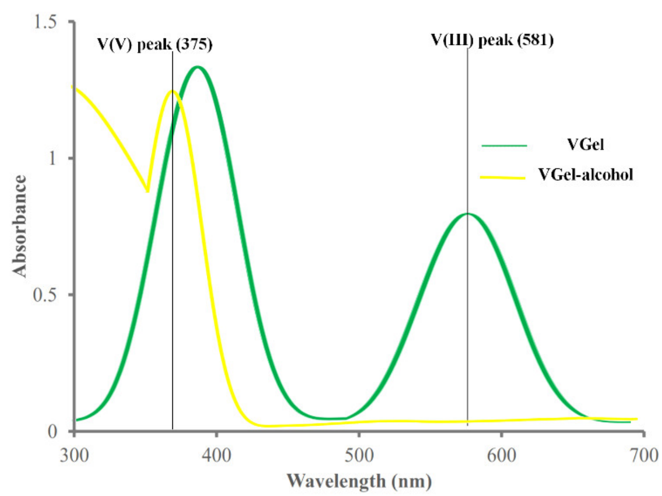

Fig. S12. The UV-Visible absorption spectrum of (a) VGel and (b) VGel in the presence of EtOH/MeOH (40/6%) for 2.5 min [S11].

Furthermore, some literatures survey disclosed the reduction possibility of $V^{IV}O^{2+}$ complexes to V^{III} species. This reduction is almost quantitatively and happened easily in the presence of some organic ligands with neither catalyst nor heat [S12]. In this study, when the reaction was run in the absence of BTC, only a clear yellow solution (no green precipitations nor green metallogel) was obtained. Thus, it could be concluded that $V^{IV}O^{2+}$ specie in the presence of BTC gelator, leads to the formation of a dark green metallogel of V^{III} in a very high yield □ 85%.

Rheological properties

The rheological behavior of the VGel was also studied. In the frequency sweep experiment, the measured storage modulus (G′) values were significantly greater than the loss modulus (G″) and the linear response confirmed the elastic behavior of the metallogel (Fig. S11).

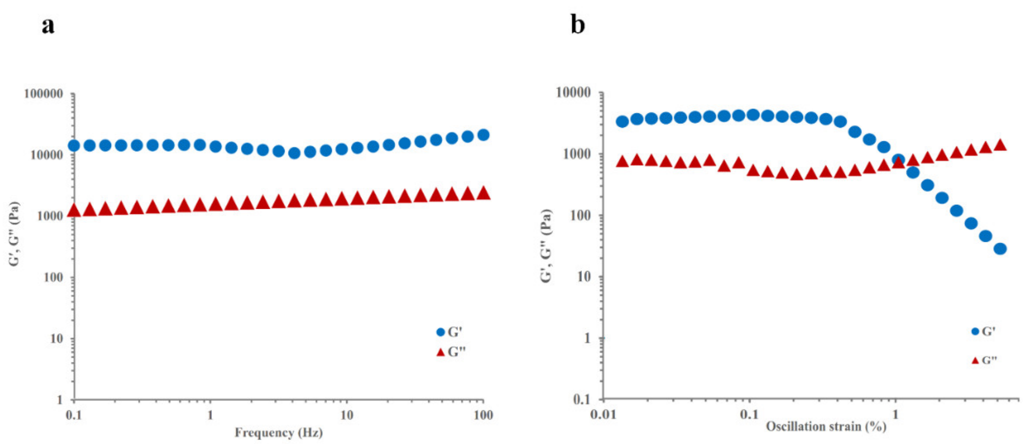

Fig. S13. a) Dynamic frequency sweep rheometry data with strain kept at 0.4% b) Strain sweep rheometry data with frequency kept at 0.1 Hz

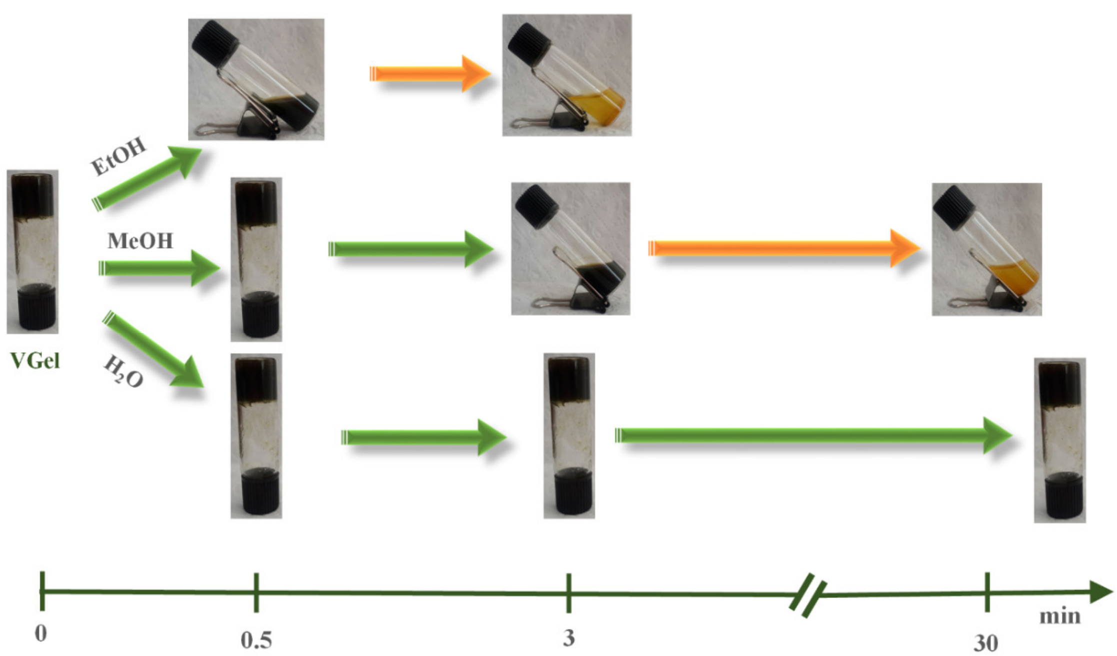

Fig. S14. Solvent stimuli-response of VGel

Self-healing

To test the self-healing properties, the VGel treated with external mild mechanical stress by vortex for 5 min at 100 rpm. In response VGel lost its integrity to stable green pieces without any marked visible change after a couple of months. In addition, the resulted dark-green pieces doesn't show any reconstitution behavior also after 24 hours, as expected from a colloidal gel that its self-assembly directed by weak interactions is demonstrated in computational sections (Fig. S13).

Fig. S15. Self-healing of VGel

References

[S1] L. Martinez, R. Andrade, E. G. Birgin, J. M. Martinez, PACKMOL: A Package for Building Initial Configurations for Molecular Dynamics Simulations. J. Comput. Chem. 30 (2009) 2157–2164.

[S2] N. Zhang, B. Yang, J. Huo, W. Qi, X. Zhang, X. Ruan, J. Bao, G. He, Hydration Structures of Vanadium/Oxovanadium Cations in the Presence of Sulfuric Acid: A Molecular Dynamics Simulation Study. Chem. Eng. Sci. 195 (2019) 683–692.

[S3] E. Wernersson, P.. Jungwirth, Effect of Water Polarizability on the Properties of Solutions of Polyvalent Ions: Simulations of Aqueous Sodium Sulfate with Different Force Fields. J. Chem. Theory Comput. 6 (2010) 3233–3240.

[S4] W. R. Cannon, B. M. Pettitt, J. A. McCammon, Sulfate Anion in Water: Model Structural, Thermodynamic, and Dynamic Properties. J. Phys. Chem. 98 (1994) 6225–6230.

[S5] A. Tahli, U. Koc, R. Elshaarawy, A. Kautz, C. Janiak, A Cadmium Anionic 1-D Coordination Polymer $\{[Cd(H_2O)_6][Cd_2(atr)_2(\mu_2\text{-}btc)_2(H_2O)_4]2H_2O\}_n$ within a 3-D Supramolecular Charge-Assisted Hydrogen-Bonded and π-Stacking Network. Crystals. 6 (2016) 23-32.

[S6] A. Gladysiak, T.N. Nguyen, J. A. R. Navarro, M. J. Rosseinsky, K. C. Stylianou, A Recyclable Metal–Organic Framework as a Dual Detector and Adsorbent for Ammonia. Chem. Eur. J. 23 (2017) 13602–13606.

[S7] G. Yu, X. Yan, C. Han, and F. Huang, Characterization of supramolecular gels. Chem. Soc. Rev. 42, (2013) 6697-6722.

[S8] L. E. Orgel, Spectra of transition□metal complexes. J. Chem. Phys. 23 (1995) 1004-1014.

[S9] C. Choi, S. Kim, R. Kim, Y. Choi, S. Kim, H. Y. Jung, and H. T. Kim, A review of vanadium electrolytes for vanadium redox flow batteries. Renew. Sustain. Energy Rev. 69 (2017) 263-274.

[S10] R. P. Brooker, C. J. Bell, L. J. Bonville, H. R. Kunz, and J. M. Fenton, Determining vanadium concentrations using the UV-Vis response method. J. Electrochem. Soc. 162 (2015) A608-A613.

[S11] N. H. Choi, S. K. Kwon, and H. Kim, Analysis of the oxidation of the V (II) by dissolved oxygen using UV-visible spectrophotometry in a vanadium redox flow battery. Journal of the Electrochem. Soc., 160 (2013) A973.

[S12] M. J. Manos, A. J. Tasiopoulos, C. Raptopoulou, A. Terzis, J. D. Woollins, A. M. Slawin, and T. A. Kabanos, Unexpected reduction of vanadium (IV) to vanadium (III) in the presence of the chelate ligands 2, 2′-bipyridine (bpy) and 1, 8-hydroxyquinoline (Hquin). Dalton Trans. 10 (2001) 1556-1558.